water

MDPI

Article

Combination of a Highly Efficient Biological System and Visible-Light Photocatalysis Pretreatment System for the Removal of Phthalate Esters from Wastewater

Chih-Yu Chen [1], Guey-Horng Wang [2,*], Yu-Jen Chang [3], Yi-Hui Chen [3], Chiu-Yu Cheng [3] and Ying-Chien Chung [3,*]

[1] Department of Tourism and Leisure, Hsing Wu University, New Taipei City 244012, Taiwan
[2] Research Center of Natural Cosmeceuticals Engineering, Xiamen Medical College, Xiamen 361008, China
[3] Department of Biological Science and Technology, China University of Science and Technology, Taipei City 115311, Taiwan
* Correspondence: 201400080001@xmmc.edu.cn (G.-H.W.); ycchung@cc.cust.edu.tw (Y.-C.C.); Tel.: +886-22782-1862 (Y.-C.C.); Fax: +886-22786-5456 (Y.-C.C.)

Abstract: To save energy and increase treatment efficiency, a visible-light photocatalysis system was coupled with a biological treatment system for the continuous removal of phthalate esters (PAEs) from synthetic wastewater. Di-(2-ethylhexyl) phthalate (DEHP), dibutyl phthalate (DBP), and dimethyl phthalate (DMP) were treated using an iodine-doped TiO_2 photocatalyst, and the reactions followed first-order kinetics (similar to ultraviolet TiO_2 photocatalysis) to produce phthalic acid as an intermediate product. The effects of various operating factors, such as PAE concentrations, pH, light intensity, retention time (RT), and the coexistence of PAEs, on individual PAE removal were investigated. DEHP-degrading bacteria were isolated from DEHP-contaminated soil, purified through serial dilution, and then identified through DNA sequencing. The results indicated that the optimal operating conditions for PAE removal with a visible-light photoreactor were a pH of 5, a temperature of 30 °C, a light intensity of 300 W, and an RT of 5.5 min. DEHP, which contains long and branched chains, was more difficult to degrade than DMP, which contains short alkyl side chains. *Pseudomonas* sp. was the most dominant bacteria in the DEHP-contaminated soil and was inoculated in a packed bed reactor (PBR) for complete PAE degradation. The effluent containing PAEs was pretreated using the visible-light photoreactor under a short RT. This treatment resulted in the effluent becoming biodegradable, and PAEs could be completely removed from the treated effluent by using the PBR. The coupled photobiological system achieved removal efficiencies of 99.6%, 99.9%, and 100% for DEHP, DBP, and DMP, respectively, during the continuous treatment. The results of this study indicate that the developed coupled system is an effective, energy-saving, and cost-efficient tool for treating wastewater containing PAEs.

Keywords: photocatalysis; phthalate esters; packed bed reactor; titanium dioxide

Citation: Chen, C.-Y.; Wang, G.-H.; Chang, Y.-J.; Chen, Y.-H.; Cheng, C.-Y.; Chung, Y.-C. Combination of a Highly Efficient Biological System and Visible-Light Photocatalysis Pretreatment System for the Removal of Phthalate Esters from Wastewater. *Water* **2022**, *14*, 3139. https://doi.org/10.3390/w14193139

Academic Editor: Alexandre T. Paulino

Received: 27 August 2022
Accepted: 30 September 2022
Published: 5 October 2022

1. Introduction

Phthalate esters (PAEs) contain a diverse group of chemicals and play a key role in various commercial, industrial, and medical applications [1]. PAEs might leak into the environment from plastic products. PAEs are currently listed as priority pollutants and endocrine-disrupting compounds in several countries because of their link to several cancers [2]. Because they are priority pollutants, the PAE risks are assessed and attempts are made to reduce their production to control phthalate pollution. Some studies have reported the presence of PAEs in sludge and solid wastes, and PAEs are ubiquitous as environmental and food contaminants because they leach easily [3,4]. PAEs are composed of a variety of compounds with various structures and properties. The most abundant PAE in the environment is di-(2-ethylhexyl) phthalate (DEHP). DEHP is listed as a priority pollutant by

the U.S. Environmental Protection Agency and the European Union [5]. Dibutyl phthalate (DBP) and dimethyl phthalate (DMP) are also common PAEs [6,7].

PAEs can be degraded by microbes under various conditions [8]. However, the biodegradation process is time-consuming when reducing PAE concentrations to a harmless level [9,10]. Furthermore, PAEs are difficult to remove using conventional water treatment processes, such as coagulation, sedimentation, filtration, and disinfection, because PAEs are biorecalcitrant and have low photodegradability [11]. Thus, developing an effective and efficient method for PAE removal is vital. Advanced oxidation processes (AOPs) have been proposed as a potential alternative approach for treating biorecalcitrant organic pollutants [12]. One of the most promising AOPs is TiO_2 photocatalysis. However, the high energy demand for the complete mineralization of PAEs makes AOPs inefficient [13]. Consequently, to increase the efficiency and effectiveness of PAE treatment, AOPs are usually combined with biological processes [14]. In addition to PAEs, some heavy metal pollutants could be removed through adsorption or desorption methods [15]. Regarding photocatalysis, some investigations have been conducted on the degradation of PAEs under ultraviolet (UV) or sunlight irradiation by using TiO_2 photocatalysis [2]. However, the large bandgap energy of TiO_2 (3.2 eV) restricts its photocatalytic applications to the UV range. Therefore, to ensure that electromagnetic radiation across the solar spectrum is used effectively in photocatalysis, visible light is introduced into the TiO_2 matrix to extend the photoresponse range [16]. An iodine (I)-doped TiO_2 photocatalyst is highly efficient in decomposing pollutants under visible-light irradiation [17]. However, no study has used visible-light photocatalysis pretreatment and a biological system to remove PAEs efficiently from effluents.

Our study evaluated the efficiency of a visible-light-driven photocatalytic degradation system in removing PAEs from wastewater and the biodegradability of the treated solutions and effluents under a short retention time (RT). The effects of PAE concentration, pH, light intensity, RT, and the coexistence of PAEs in the photocatalytic system on the efficiency of removing individual PAEs were also evaluated. Furthermore, the compositions of the intermediate products in the photocatalytic pretreatment system were analyzed. Biodegradation was performed in a packed bed reactor (PBR) inoculated with a PAE-degrading strain to evaluate the feasibility of the developed coupled system (combination of a visible-light photocatalysis system and biological treatment system).

2. Materials and Methods

2.1. Materials

Analytical grade DEHP, DBP, DMP (purity = 99%), and titanium tetraisopropoxide (TTIP) (purity = 98%) were purchased from AccuStandard (New Haven, CT, USA). A neutral pH for the biological experiment was maintained automatically by using 0.1 M HCl or 0.1 M NaOH in a storage tank. PAE (DEHP, DBP, and DMP) stock solution (100 mg/L) was serially diluted to the desired concentrations, and 0.1 mL of polysorbate 80 (TWEEN 80, Sigma-Aldrich, St. Louis, MO, USA) was added to increase the solubility. The mineral medium (g/L) contained KH_2PO_4, 1.09; K_2HPO_4, 2.10; $(NH_4)_2SO_4$, 0.40; $CaCl_2$, 0.29; $MgSO_4$, 0.21; $MnSO_4$, 0.21; and $FeSO_4$, 0.02. All culture media, biochemical reagents, and chemicals were purchased from Sigma-Aldrich (St. Louis, MO, USA) unless otherwise stated. Furthermore, we used glassware rather than plasticware to avoid possible PAE contamination.

2.2. Synthesis of I-Doped TiO_2

I-doped TiO_2 was synthesized using a modified version of the method of Štengl and Grygar [16] and Hung et al. [10]. First, 0.89 mL of TTIP was mixed with 10 mL of isopropanol solution (0.3 M). This mixture was stirred for 30 min and then slowly dipped once with distilled water and alcohol until the hydrogel solution was cloudy. Subsequently, 35% HCl was added to the solution, and the solution pH value was adjusted to 3–4 until the solution transformed into a white transparent gel. A total of 100 mL of the transparent gel

was mixed with 100 mL of 30% H_2O_2 solution to produce a yellow gelatinous mass. This mass was mixed with 0.7 g of KI and heated at 80 °C until a yellowish-white precipitate formed. After cooling for 30 h, the color of the precipitate changed to white, and I-doped TiO_2 power was obtained.

2.3. Preparation of I-Doped TiO_2-Coated Beads, Design of the Photoreactor, and Photocatalysis of PAEs

First, 0.5 g of I-doped TiO_2 was mixed with a 1 mL solution containing 0.1 mL of acetylacetone and then mildly stirred to produce a viscous paste. Subsequently, the paste was added to 1.7 mL of distilled water and 0.05 mL of Triton X-100 and then mixed with 15 g of silica glass beads (internal diameter [ID] = 2 cm). Second, the beads coated with I-doped TiO_2 were removed from the liquid by heating for 10 min at 80 °C and then further heating for 30 min at 450 °C in an oven to immobilize the I-doped TiO_2. The concentration, specific surface area, and crystal size of the I-doped TiO_2 on the surface of the glass beads were 0.38%, 205 m^2/g, and 29.8 nm, respectively.

The concentric cylindrical photoreactor (length = 50 cm, ID = 7 cm) comprised an inner cylinder (ID = 5 cm) with an exterior surrounded by glass material. The light source of the photoreactor was a xenon lamp with a variable power supply (100–500 W), and the lamp was placed on the inner cylinder. The I-doped TiO_2-coated beads were packed in the outer cylinder of the photoreactor (packing height = 30 cm, packing volume = 565 mL). A solution containing PAEs was introduced into the photoreactor in an upward flow mode by using a peristaltic pump.

To evaluate the basic characteristics of batch PAE photocatalysis, a petri dish (ID = 9 cm) was packed with I-doped TiO_2-coated beads and 40 mg/L of PAEs (total volume = 31.8 mL). A xenon lamp with an intensity of 200 W was used to irradiate the area located 5 cm above the petri dish continuously at 30 °C. Changes in PAE concentration were recorded every 5 min for 60 min, and the reaction kinetics were analyzed. To evaluate the characteristics of continuous PAE photocatalysis, the concentric cylindrical photoreactor was used. Experiments were performed at various pH levels (2–10), PAE concentrations (0.1–50 mg/L), light intensities (200–400 W), RTs (4–7 min), and PAE mixture compositions to evaluate the effects of these parameters on the efficiency of PAE removal. PAEs were continuously fed into the photoreactor from the illumination part of the system. Unless otherwise stated, the operating conditions were as follows: pH = 5.0, temperature = 30 °C, RT = 5.5 min, and light intensity = 300 W. Effluents were continuously collected for 30 min, and the PAE concentration was determined using high-performance liquid chromatography (HPLC). The PAE removal efficiency was calculated as the average PAE removal efficiency over a 30 min operation time.

2.4. Screening, Identification, and Degradation Characteristics of DEHP-Degrading Bacteria

The DEHP-degrading bacteria were isolated from the soil. Soil samples were taken randomly from several locations near a plastic factory in Tainan City, Taiwan, at a depth of 10 cm from the topsoil. Soil samples were sequentially mixed with increasing DEHP concentrations (20–100 mg/L) and then acclimated for 7, 14, 18, and 21 days. The residual concentration of DEHP in the soil was analyzed. The denaturing gradient gel electrophoresis (DGGE) method was used to analyze the bacterial community in the soil (Section 2.7). To determine the dominant DEHP-degrading strains, the slurries of soil that were acclimated to DEHP (100 mg/L) after 21 days were serially diluted and plated on tryptone soy agar to isolate the culturable strain. Subsequently, the dominant bacterial colonies were individually identified through DNA sequencing until the isolate was the same as the dominant strain found in the DGGE method (i.e., the band with the brightest intensity).

To evaluate the characteristics of the DEHP-degrading strain when degrading various PAEs, the isolate was enriched in tryptone soy broth for 24 h. The batch PAE degradation experiment was conducted in a 300 mL conical flask. The DEHP-degrading strain was inoculated into a mineral medium containing 10 mg/L of PAEs (pH 7) to achieve a final

cell concentration of 10^8 CFU/mL. The effects of pH (6.0–8.5), temperature (20–45 °C), reaction time (24 h), and the coexistence of PAEs (mixture of DEHP and DBP; mixture of DMP and DEHP; mixture of DMP and DBP; and mixture of DEHP, DBP, and DMP) on PAE removal were evaluated. Unless otherwise stated, the operating conditions were a pH of 7.0, a temperature of 30 °C, and a degradation time of 24 h.

2.5. Bioreactor (PBR) Design and Immobilization Procedure

A cylindrical PBR (length = 150 cm, ID = 20 cm) was constructed from acrylic material. Two pores were established at the top of the PBR for pH and dissolved oxygen measurements. Wastewater containing PAEs or intermediates from the photoreactor outlet was poured into the storage tank and introduced into the PBR in an upward flow mode.

The immobilization procedure of the DEHP-degrading strain is described in the following text. First, a 2.5 L packed volume of plastic Raschig rings (rosette type; ID = 2 cm) was positioned in the PBR as packing material. Second, the inflow solution containing the DEHP-degrading strain (2×10^8 CFU/mL) and the Luria–Bertani broth was continuously introduced into the PBR under an RT of 24 h for 2 weeks. Before the experiment, the blank test revealed that no PAEs were detected in the Raschig rings.

2.6. Coupled Photobiological System Design

The coupled visible-light photobiological system developed in this study consisted of a concentric cylindrical photoreactor, PBR, storage tank, peristaltic pump, and connecting tube (Figure 1). Wastewater containing a PAE mixture (each mixture of DEHP, DBP, and DBP had a concentration of 50 mg/L) was continuously introduced into the photoreactor. The parameter settings of the photoreactor were the same as those in Section 2.3. Before the effluent was poured into the PBR, the pH value of the effluent was automatically adjusted to 7 in the storage tank, and the effluent was then pumped to the PBR using a peristaltic pump under an RT of 4 h. The mineral medium was added to maintain the microbial activity in the PBR if required. The coupled system was continuously operated for 6 h, and the 6 h average efficiency of removing PAEs was noted.

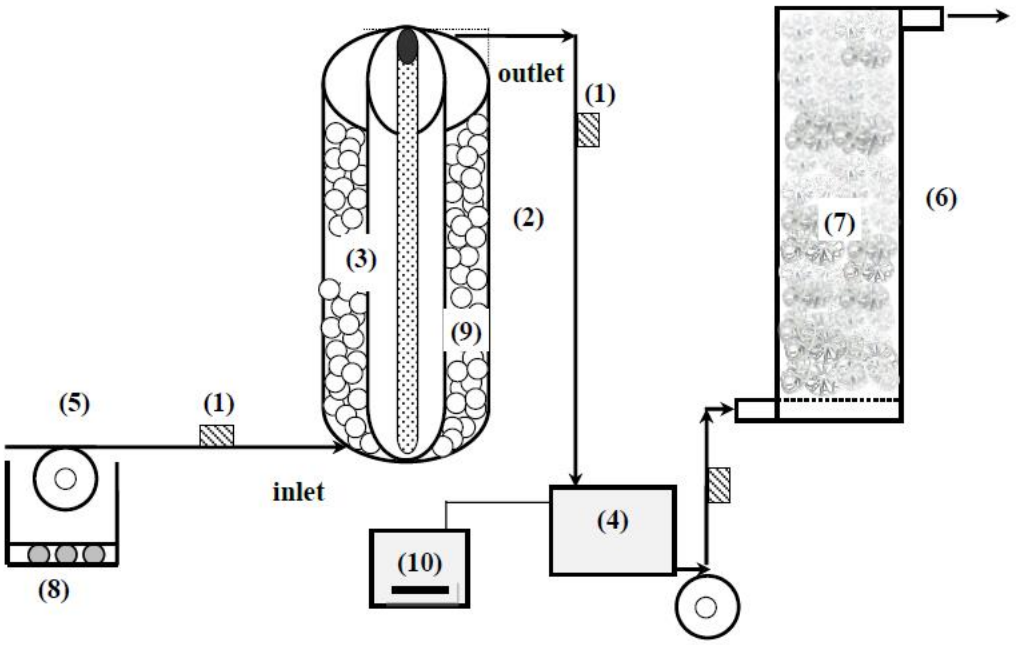

Figure 1. Schematic of the developed coupled photobiological system. (1) Fluid flowmeter, (2) concentric cylindrical photoreactor, (3) xenon lamp, (4) storage tank, (5) peristaltic pump, (6) cylindrical PBR, (7) plastic Raschig rings, (8) stirring machine, (9) I-doped TiO_2-coated beads, and (10) pH controller.

2.7. Chemical and Biological Analysis

To analyze the PAE concentration, we used an HPLC system (Hitachi, Tokyo, Japan), which comprised two Hitachi L-6000 pumps, one L-5000 liquid chromatography controller, and one Hitachi L-4200 UV–visible detector at 280 nm. HPLC separation was performed using a C18 column (4.6 mm ID × 250 mm, 5 μm). The mobile phase was isocratic $CHCl_3$:C_6H_{14} (3:7), and the flow rate was 1 mL/min. The biochemical oxygen demand (BOD_5) was measured using an OxiTop-i IS 6 system (WTW, Weilheim, Germany). The chemical oxygen demand (COD) was analyzed using a HACH DR2800 portable spectrophotometer (Hach, Loveland, CO, USA). The intermediate products of PAE photocatalysis were first extracted through solid-phase extraction and evaporated into vials. The extract was dissolved in a small volume of chloroform and then injected into a gas chromatography–mass spectrometry (GC–MS) instrument (injection amount: 0.5 μL). The GC–MS instrument comprised an HP 5890 series II gas chromatograph and an HP 5971 mass spectrometer (Agilent, Santa Clara, CA, USA). GC separation was performed using an Ultra-2 fused silica capillary column (0.2 mm ID × 25 m) in a temperature range of 100–280 °C. Helium was used as the carrier gas, and the gas flow rate was 31 cm/s. The injector and detector temperatures were set as 250 and 280 °C, respectively. The analysis of intermediate products was conducted in the EI mode at 70 eV under a full-scan setting. The electron impact mass spectrum of DEHP indicated that the molecular ion was detected at m/z 390 and other important ions were detected at m/z 279, 167, and 149 (base peak). DBP demonstrated the molecular ion at m/z 278 and other important ions at m/z 223, 205, 167, and 149 (base peak). DMP exhibited the molecular ion at m/z 194 and other important ions at m/z 167 and 149 (base peak).

To analyze the change in the soil bacterial communities during the acclimatization period, a Bio-Rad DGGE system (Hercules, CA, USA) with a Bio-Rad imaging program (Quantity One 4.5.2) was applied. Cell lysis, DNA extraction, and polymerase chain reaction amplification were conducted according to the methods of Chen et al. [18]. The segment of eubacterial 16S rDNA was amplified with the primer pair F968GC and R1401. The DNA samples were run on an 8% acrylamide gel with a 45%–60% denaturant gradient at a constant voltage of 100 V for 16 h at 60 °C. The resulting gels were stained with ethidium bromide for 20 min. Representative bands were identified by excising bands from the DGGE gel and then eluting, reamplifying, and sequencing them. The obtained sequences were compared with those in GenBank by using the BLAST program to determine the closest known relatives according to the partial 16S rRNA gene homology.

3. Results and Discussion

3.1. Degradation Kinetics of PAEs and Effects of PAE Concentration in the Photoreactor on Removal Efficiency

The photocatalytic reaction of PAEs usually follows first-order kinetics and can be described as follows:

$$\frac{d(PAEs)}{dt} = -k(PAEs)_0, \quad (1)$$

where t is the irradiation time, k is the reaction rate constant, $PAEs_0$ is the initial concentration of PAEs (mg/L), and $PAEs$ is the concentration of PAEs at time t (mg/L). In the present study, the degradation kinetics of PAEs were examined in batch experiments, and degradation rates were highly reproducible, with r^2 being equal to 0.9912 for the plots of the natural log of the DEHP concentration versus time ($y = 0.0562x$). The rate constant of the visible-light photocatalytic degradation was 0.0562 1/min. Similarly, the rate constants for DBP and DMP were 0.0618 and 0.0972 1/min, respectively. Therefore, the order of the PAEs in terms of their reaction rate was as follows: DMP > DBP > DEHP. Consequently, the photocatalytic reaction rate was negatively correlated with the structural complexity of PAEs. The reaction rate of the visible-light-assisted, I-doped TiO_2 photocatalysis for DEHP was higher than that (0.0003 1/min) of UV-assisted TiO_2 photocatalysis in our previous study [19].

Figure 2 depicts the effects of PAE concentration on the efficiency of removing PAEs in a continuous treatment with the visible-light photoreactor. The results indicated that the removal efficiency considerably decreased when the PAE concentration increased from 10 to 50 mg/L. Zhang et al. observed that a lower PAE concentration can react with higher abundances of · OH, which results in a higher PAE removal efficiency [20]. Consequently, the removal efficiency is negatively affected by an increase in PAE concentration. At 50 mg/L, the DEHP, DBP, and DMP removal efficiencies were 81.5% ± 1.2%, 85.8% ± 0.8%, and 96.8% ± 1.5%, respectively. At 5 mg/L, the efficiency of removing PAEs reached 100%. The results of Xu et al. (2010) indicated that the DBP and DMP removal efficiencies at 5 mg/L were only 98% and 80%, respectively, in a PW_{12}–TiO_2-simulated sunlight system [2]. We hypothesize that completely removing PAEs, especially DEHP with a complex structure, under a short RT (e.g., 5.5 min) through only photocatalysis is difficult. Associated chemical and biological characteristics, such as the BOD_5/COD ratio, were measured to assess the effect of visible-light photocatalysis on the biodegradability of synthetic wastewater. Table 1 lists the BOD_5/COD ratios of PAE-containing wastewater that was treated using the visible-light photoreactor. The results indicated that the higher the inlet PAE concentration, the lower the BOD_5/COD ratio and, thus, the biodegradability of effluents. In general, when the inlet PAE concentration was >40 mg/L, the biodegradation index (BOD_5/COD) of the effluent of the photoreactor was ≤0.4. PAE-degrading bacteria might be required in a subsequent biological system to achieve 100% PAE removal in the event of a high PAE concentration.

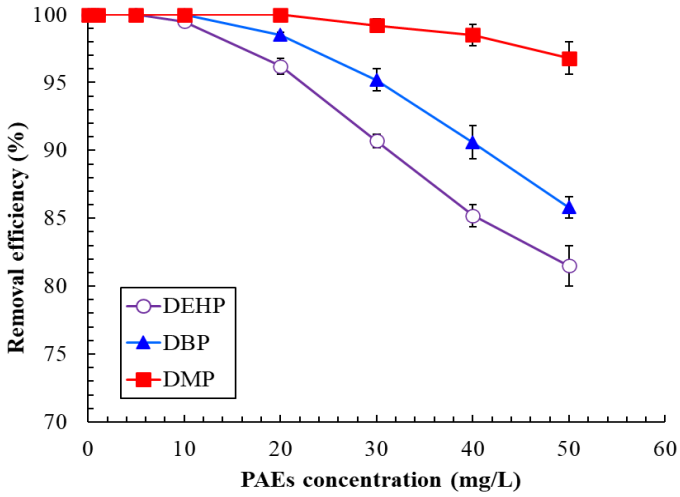

Figure 2. Effect of the initial PAE concentration on the continuous removal of PAEs from synthetic wastewater introduced into the visible-light photoreactor. PAE concentration: 0.1 to 50 mg/L; light intensity: 300 W; pH: 5.0; temperature: 30 °C; and RT: 5.5 min.

Table 1. Effect of visible-light photocatalysis on the biodegradability (BOD_5/COD) of PAEs. The PAE concentration ranged from 10 to 50 mg/L.

	10	**20**	**30**	**40**	**50**
DEHP	0.71	0.68	0.51	0.45	0.35
DBP	0.72	0.7	0.58	0.51	0.38
DMP	0.75	0.72	0.65	0.56	0.41

3.2. Effects of pH, RT, and Light Intensity on PAE Removal Efficiency of the Photoreactor

The results indicated that pH had a nonsignificant effect on the PAE removal efficiency (>99.5% at a PAE concentration of 40 mg/L) between pH values of 2 and 4 ($p > 0.05$). However, an increase in the pH of the inlet wastewater containing PAEs led to a clear

decrease in their removal efficiency when the pH was 5–6 (Figure 3a). The removal efficiency gradually increased when the pH was ≥8. Although higher PAE removal efficiencies were observed at pH values of 2–4 than at other pH values, the acidic environment at pH values of 2–4 would affect the microbial activity in the PBR. Thus, the pH for the photocatalysis pretreatment was set to 5 to ensure suitable conditions for the microbial degradation system. Under this condition, the DEHP, DBP, and DMP removal efficiencies were 85.2% ± 1.2%, 90.6% ± 0.6% and 98.5% ± 0.3%, respectively.

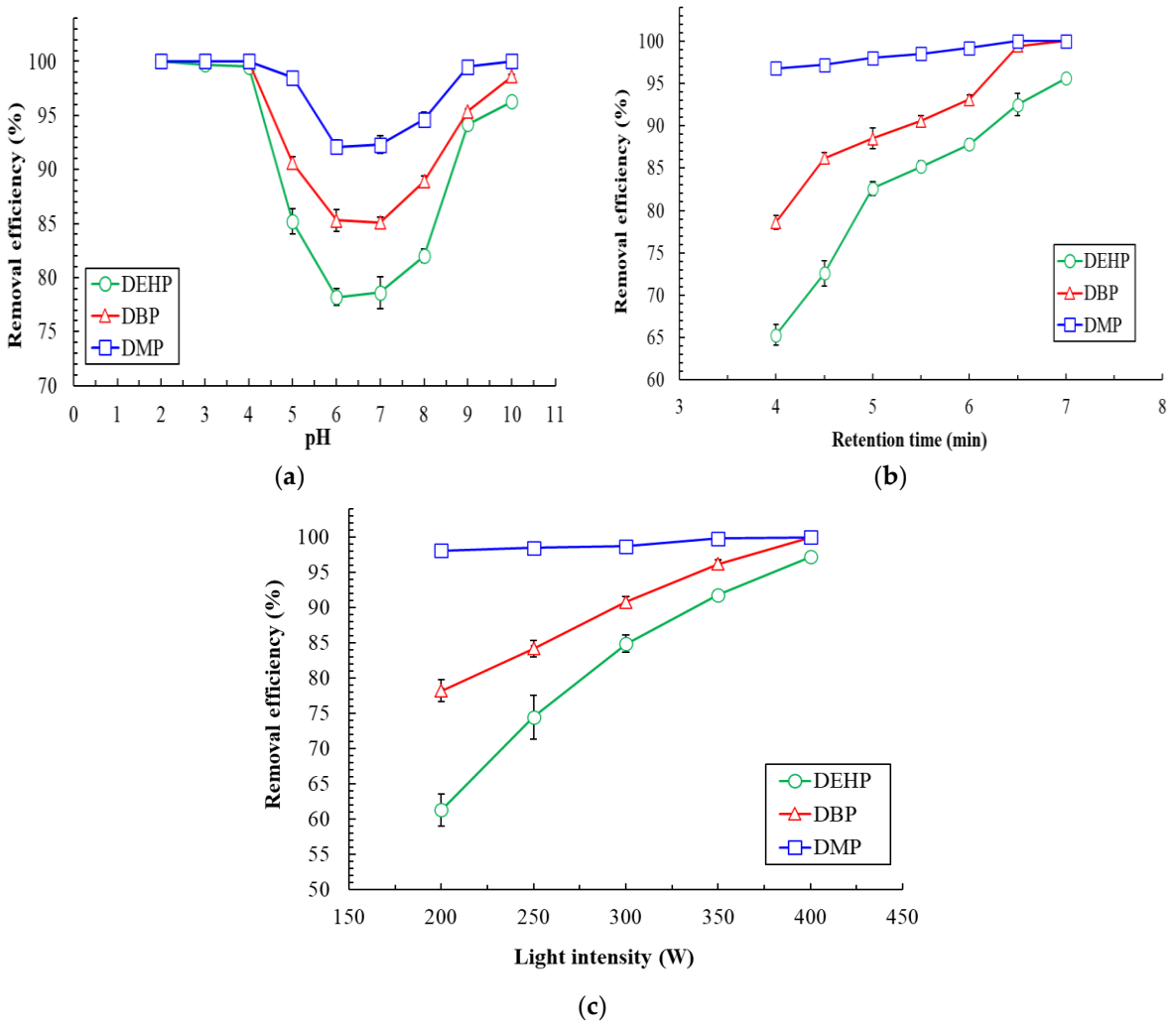

Figure 3. (**a**) Effect of the pH on the continuous removal of 40 mg/L of PAEs from synthetic wastewater introduced into the visible-light photoreactor. Light intensity: 300 W; temperature: 30 °C; and RT: 5.5 min. (**b**) Effect of the RT on the continuous removal of 40 mg/L of PAEs from synthetic wastewater introduced into the visible-light photoreactor. Light intensity: 300 W; temperature: 30 °C; and pH: 5.0. (**c**) Effect of the light intensity on the continuous removal of 40 mg/L of PAEs from synthetic wastewater introduced into the visible-light photoreactor. Temperature: 30 °C; RT: 5.5 min; and pH: 5.0.

The RT of the wastewater containing PAEs in the visible-light photoreactor varied between 4 and 7 min. The highest removal efficiency (95.6% ± 0.6%) of DEHP at 40 mg/L occurred under an RT of 7 min. The DMP and DBP removal efficiencies were 100% under an RT of 7 min (Figure 3b). Therefore, in the photoreactor, the longer the liquid RT (i.e., the lower the flow rate) of wastewater, the higher the PAE removal efficiency. However, the effect of RT on PAE removal varied depending on whether the PAEs were easily photolyzed [1]. Among the PAEs, the aforementioned effect yielded the highest and lowest removal efficiencies for DMP and DEHP, respectively. In general, the PAE removal rate

of the biodegradation system was lower than that of the photocatalysis system. Thus, a reasonable RT of 5.5 min was adopted to achieve a satisfactory PAE removal efficiency and a low volume in the storage tank. The developed coupled system outperformed the photo-Fenton pretreatment system developed in our previous study, which had a RT of up to 36 min [14].

Figure 3c shows how the recalcitrant DEHP and DBP removal efficiencies increased significantly in a linear manner with the visible-light intensity. DMP removal also increased, but nonsignificantly. Therefore, a higher light intensity excited the I-doped TiO_2 catalyst to generate more free radicals [19]. Because of financial considerations, the optimal light intensity for PAE photocatalytic degradation was 300 W. Consequently, the removal efficiencies for 40 mg/L of DEHP, DBP, and DMP were 84.9% ± 1.2%, 90.8% ± 0.8%, and 98.7% ± 0.2%, respectively. However, the removal efficiency for 10 mg/L of DEHP was 89% in a visible-light photoreactor (300 W) when using a Z-scheme Bi_2O_3/TiO_2 catalyst [21].

3.3. Effect of Coexisting PAEs on PAE Removal in the Visible-Light Photoreactor

In a real wastewater environment, PAEs are usually a mixture of multiple pollutants [22]. To understand the effect of coexisting PAEs on individual PAE removal, the DEHP, DBP, or DMP removal efficiencies from the PAE mixtures were analyzed using a photoreactor. The concentration of each PAE in the mixture was set to 20 mg/L. As displayed in Figure 4, the DEHP and DBP removal efficiencies were considerably affected by the coexistence of PAEs. The removal efficiencies for DEHP (86.5% ± 1.2%) and DBP in the mixture (92.3% ± 0.6%) were significantly lower than the DEHP and DBP removal efficiencies in separate solutions at the same concentration (96.2% ± 0.2% and 98.5% ± 0.3%, respectively) (Figure 2). However, the effect of PAE coexistence on the DMP removal efficiency, which has a simple chemical structure, was minimal. Therefore, PAE mixtures in wastewater affect the removal efficiencies for ecalcitrant DEHP and DBP.

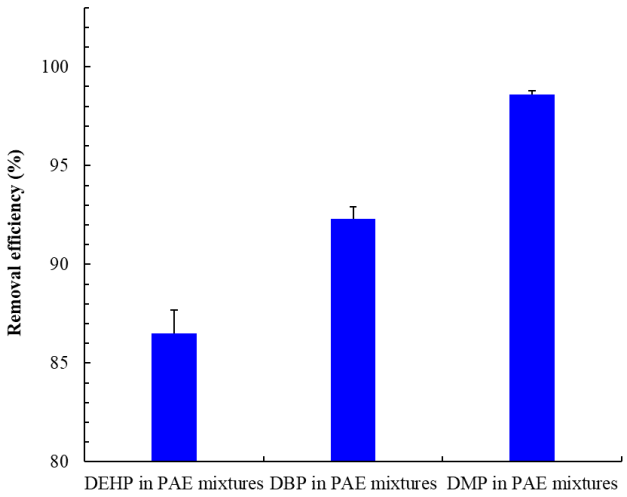

Figure 4. Effect of the coexistence of PAEs on the continuous removal of PAEs from synthetic wastewater that contains a mixture of PAEs (20 mg/L of DEHP, DBP, and DMP) and is introduced into the visible-light photoreactor. Light intensity: 300 W; temperature: 30 °C; pH: 5.0; and RT: 5.5 min.

3.4. Analysis of the Intermediate Products in the Visible-Light Pretreatment System

HPLC and GC–MS analyses were performed to identify the PAE compounds and their intermediate products in the visible-light-pretreated effluent. Sampling began 30 min after initiating the visible-light pretreatment system, and the molecular ion and fragment peaks were compared with GC–MS data stored in the National Institute of Standards and Technology (NIST) library. The similarities between the intermediates and NIST standards ranged from 96.7% to 99.5%. The UV photocatalytic degradation pathways of DBP and DEHP were investigated by Kaneco et al. [23] and Chung and Chen [19], respectively.

A comparison of their results with those of our study on DEHP, DBP, and DMP revealed that the only intermediate product common to the photochemical degradation of PAEs was phthalic acid. Furthermore, the formation of monomethyl phthalate, monobutyl phthalate, and mono-2-ethylhexyl phthalate indicated that the oxidation of the aliphatic chain was a common initiating pathway for the formation of these three PAEs. Moreover, although the light sources used in the three studies were different, they had a limited effect on the pathways of PAE photocatalysis.

3.5. Changes in the Bacterial Community of the Soil and the Degradation Characteristics of DEHP-Degrading Bacteria

Figure 5a shows the DGGE profiles of the bacterial community in the soil. The bacterial community was sequentially acclimated to various DEHP concentrations. We observed a change in the bacterial community structure, and the complexity of the DGGE bands exhibited a decreasing trend when DEHP concentrations increased in the soil. When DEPH was not added to the soil, 36 discriminable DGGE bands were identified. When the DEHP concentration increased from 20 to 100 mg/L, the number of discriminable DGGE bands decreased stepwise to 35 (20 mg/L), 31 (40 mg/L), 20 (60 mg/L), 16 (80 mg/L), and 10 (100 mg/L). When 100 mg/L of DEHP was in the soil, only two significantly distinguishable DGGE bands were observed. The dendrogram of the DGGE banding patterns in the soil indicates that the bacterial community acclimated to various DEHP concentrations (Figure 5b). When creating the dendrogram, we assumed that DGGE fingerprinting would produce a qualitative representation of the major variations in the composition of the bacterial community in the soil. The branching patterns suggested that the bacterial composition changed with the DEHP concentration. Two significant clusters of the DGGE banding patterns are shown in the dendrogram: (1) the banding pattern corresponding to the soils that contained 0, 20, and 40 mg/L of DEHP and belonged to the same cluster with 84.0% similarity and (2) the pattern corresponding to the soils that contained 60, 80, and 100 mg/L of DEHP and belonged to the same cluster with 81.2% similarity. Further analysis revealed that the pattern corresponding to the soils that contained 0 and 20 mg/L of DEHP belonged to the same subcluster with 99.1% similarity, and the pattern corresponding to the soils that contained 60 and 80 mg/L of DEHP of belonged to the same subcluster with 89.1% similarity. The aforementioned results clearly indicate that species within the same cluster tended to use DEHP in the same manner, and the DEHP concentration in the soil was the deciding factor in determining the composition of the bacterial community.

To better understand the differences in bacterial diversity among samples, we excised and sequenced discriminable bands to determine the strains, phylogeny classifications, similarities in nucleotide sequences, and relative abundance under different acclimated concentrations (Table 2). Twenty discriminable bands (A–T) were identified as members of five eubacterial phyla when feeding the bacteria DEHP at concentrations of 60, 80, or 100 mg/L. Six bands (A, D, N, P, Q, and S) were grouped with the phylum Proteobacteria, and their closest relatives exhibited homology with *Providencia* sp., *Acinetobacter lwoffii*, *Ochrobactrum anthropic*, *Pseudomonas* sp., *Burkholderia pyrrocinia*, and *Achromobacter denitrificans*, respectively. Six bands (B, C, E, F, G, and H) were clustered within the phylum Bacillota, namely *Bacillus megaterium*, *Bacillus antracis*, *Staphylococcus aureus*, *Staphylococcus gallinarum*, *Enterococcus faecalis*, and *Streptococcus* sp., respectively. Five bands (I, K, O, R, and T) were clustered within the phylum Actinomycetota, namely *Jonesia denitrificans*, *Corynebacterium nitrilophilus*, *Rhodococcus ruber*, *Mycobacterium houstonense,* and *Gordonia terrae*, respectively. Three bands (J, L, and M) were clustered within the phylum Bacteroidota, namely *Flavobacterium* sp., *Niabella ginsenosidivorans*, and *Terrimonas lutea*, respectively.

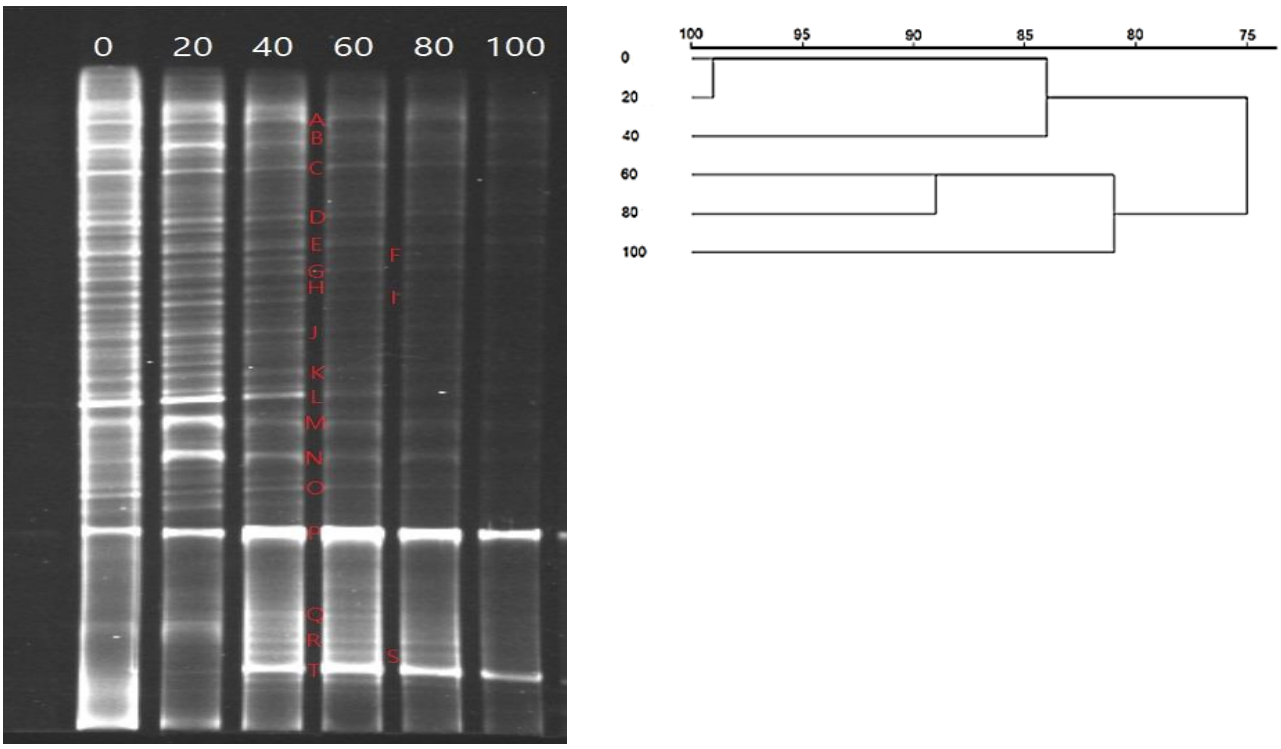

(**a**) (**b**)

Figure 5. (**a**) DGGE profiles of the bacterial community in soil sequentially acclimated to various DEHP concentrations (0–100 mg/L). (**b**) Dendrogram showing relations between DGGE banding patterns in soil when bacteria are sequentially acclimated to various DEHP concentrations.

When we summed the relative concentrations of various bacterial phyla in the acclimated soils containing 60–100 mg/L of DEHP, we found that the Proteobacteria phylum was the predominant phylum and accounted for 78.6–82.7% of all bacterial phyla. This result is consistent with the results obtained in previous studies [24]. The DGGE band results indicate that *Providencia* sp., *B. megaterium*, *B. antracis*, *A. lwoffii*, *S. aureus*, *E. faecalis*, *T. lutea*, *O. anthropic*, *Pseudomonas* sp., and *G. terrae* were consistently present at various DEHP concentrations, but *P. fluorescens* and *G. terrae* were significantly dominant. *S. gallinarum*, *Streptococcus* sp., *J. denitrificans*, *R. ruber*, *M. houstonense*, and *A. denitrificans* were present at DEHP concentrations of 20–80 mg/L, but *M. houstonense* and *A. denitrificans* were dominant. A third bacterial group that included *Flavobacterium* sp., *C. nitrilophilus*, *N. ginsenosidivorans*, and *B. pyrrocinia* was discovered exclusively at relatively low DEHP concentrations ($\leq$60 ppm). Among all the bacterial strains, *Pseudomonas* sp. was the most dominant and accounted for 71.80–81.32% of the total bacterial community in the acclimated soils that contained 60–100 ppm of DEHP. Thus, *Pseudomonas* sp. might have considerable potential for DEHP removal.

In one study, *Providencia* sp. was isolated from compost-amended soil and exhibited potential in degrading PAEs [25]. *B. megaterium* can use a wide range of PAEs as the sole carbon and energy sources for cell growth [26]. Under optimal operating conditions, *B. anthracis* can efficiently degrade DEHP over a wide concentration range [27]. Studies have revealed that *A. lwoffii* has high DEHP-degrading activity [28]. *S. aureus* and *E. faecalis* can degrade aromatic azo dye and exhibit favorable characteristics for destroying the ring structure of DEHP [29,30]. Bai et al. reported that *Terrimonas* sp. can degrade DEHP through de-esterification and β-oxidation [31]. *O. anthropi* can degrade various PAEs, including DEHP, and is consistently present in the soil at various DEHP concentrations [32]. *Pseudomonas fluorescens* can use PAEs at high concentrations as the sole source of carbon and energy [33], and *G. terrae* can degrade DEHP at high concentrations [24]. Therefore, in this study, *Pseudomonas* sp. and *G. terrae*

accounted for 71.80–81.32% and 11.60–14.32% of the total bacteria community, respectively, in the contaminated soil with 60–100 mg/L of DEHP.

Table 2. Nucleotide sequence similarity and relative abundance of the sequenced DGGE bands.

Band	Phylogeny	Closest Relatives	Relative Abundance of DGGE Bands (%)			
			Similarity (%)	60 mg/L	80 mg/L	100 mg/L
A	Proteobacteria	*Providencia* sp.	98.5	0.81	1.08	0.35
B	Bacillota	*Bacillus megaterium*	99.8	0.34	0.83	0.31
C	Bacillota	*Bacillus antracis*	98.2	0.85	0.92	0.97
D	Proteobacteria	*Acinetobacter iwoffii*	99.6	0.41	0.71	0.82
E	Bacillota	*Staphylococcus aureus*	99.6	0.46	0.72	0.76
F	Bacillota	*Staphylococcus gallinarum*	99.8	0.16	0.48	–
G	Bacillota	*Enterococcus faecalis*	98.6	0.31	0.67	0.61
H	Bacillota	*Streptococcus* sp.	99.2	0.26	0.28	-
I	Actinomycetota	*Jonesia denitrificans*	99.6	0.28	0.21	-
J	Bacteroidota	*Flavobacterium* sp.	99.3	0.42	-	-
K	Actinomycetota	*Corynebacterium nitrilophilus*	99.5	0.85	-	-
L	Bacteroidota	*Niabella ginsenosidivorans*	99.6	1.21	-	-
M	Bacteroidota	*Terrimonas lutea*	99.1	1.32	1.81	0.28
N	Proteobacteria	*Ochrobactrum anthropi*	99.8	1.40	1.98	0.26
O	Actinomycetota	*Rhodococcus ruber*	99.2	0.96	0.84	-
P	Proteobacteria	*Pseudomonas* sp.	98.2	71.80	73.71	81.32
Q	Proteobacteria	*Burkholderia pyrrocinia*	99.5	1.60	-	-
R	Actinomycetota	*Mycobacterium houstonense*	99.6	2.38	1.62	-
S	Proteobacteria	*Achromobacter denitrificans*	98.8	2.58	1.33	-
T	Actinomycetota	*Gordonia terrae*	99.5	11.60	12.81	14.32

S. gallinarum, *Streptococcus* sp., and *J. denitrificans* are responsible for degrading cyclic compounds, such as DEHP, and are present in soil over a wide DEHP concentration range [34–36]. *R. ruber*, *M. houstonense*, and *A. denitrificans* are DEHP-degrading bacteria that are relatively dominant at a DEHP concentration of 20–80 mg/L [37–39]. Studies have reported the moderate DEHP biodegradation potential of *Flavobacterium* sp., *C. nitrilophilus*, *N. ginsenosidivorans*, and *B. pyrrocinia*, which were found exclusively at relatively low DEHP concentrations in this study [31,40–42].

PAEs have alkyl side chains of various lengths. Because DEHP, which has a long alkyl chain, can be biodegraded by DEHP-degrading bacteria, PAEs with a short alkyl chain (such as DMP and DBP) can also be biodegraded. Thus, the culturable DEHP-degrading strain *Pseudomonas* sp. was adopted to evaluate the degradation characteristics of DEHP. In the batch experiments, pH marginally affected the PAE biodegradation efficiency (98.6–100%) of *Pseudomonas* sp. at a PAE concentration of 10 mg/L and a pH range of 6.5–8.0. A reaction temperature between 30 and 35 °C was suitable for PAE biodegradation (>99%) by *Pseudomonas* sp. When the PAE mixture was treated by *Pseudomonas* sp., the removal efficiency for individual PAE solutions decreased by 0.5% and 6.5% for DMP and DEHP, respectively. The degree of influence is highly related to the decomposition difficulty of each PAE. Kanaujiya et al. reported that PAE mixtures with short alkyl side chains (e.g., DMP) degraded faster under bacterial action than PAEs with long and branched chains (e.g., DEHP) [22].

3.6. PAE Mixture Removal by Using the Coupled Photobiological System

We tested the developed coupled system in the continuous mode. In a short period, we achieved partial destruction of the PAE side chains by conducting visible-light photocatalysis to increase biodegradability. According to Figure 6, the coupled photobiological system achieved removal efficiencies of 99.6%, 99.9%, and 100% for DEHP, DBP, and DMP, respectively. Thus, the PAEs were almost completely degraded. Furthermore, the photoreactor system achieved removal efficiencies of 76.2% ± 1.6%, 81.5% ± 1.2%, and 93.6% ± 0.5% for DEHP, DBP, and DMP, respectively. Therefore, the removal efficiencies achieved with the coupled photobiological system were considerably higher than those achieved with the photoreactor system alone. The DEHP removal efficiency (99.6%) for a 50 mg/L inlet mixture with the coupled system was considerably higher than that (73.1%) for a 10–35 mg/L inlet mixture with the coupled photo-Fenton pretreatment and biological system [14]. Furthermore, the complete degradation of PAEs requires diverse metabolic genes and enzymes [43]. Thus, selecting a suitable bacteria strain for the bioreactor is crucial. Zeng et al. reported that the PAE-degrading strain *P. fluorescens* can use a PAE mixture as the sole source of carbon and energy, even at a high concentration (200 mg/L) [33]. This phenomenon might explain the high efficiency of the developed system, which was inoculated with a highly efficient PAE-degrading strain. In addition, the optimal operation parameters and detailed cost–benefit evaluation of the PAE removal efficiency using the developed coupled photobiological system will be useful for successful industrial applications.

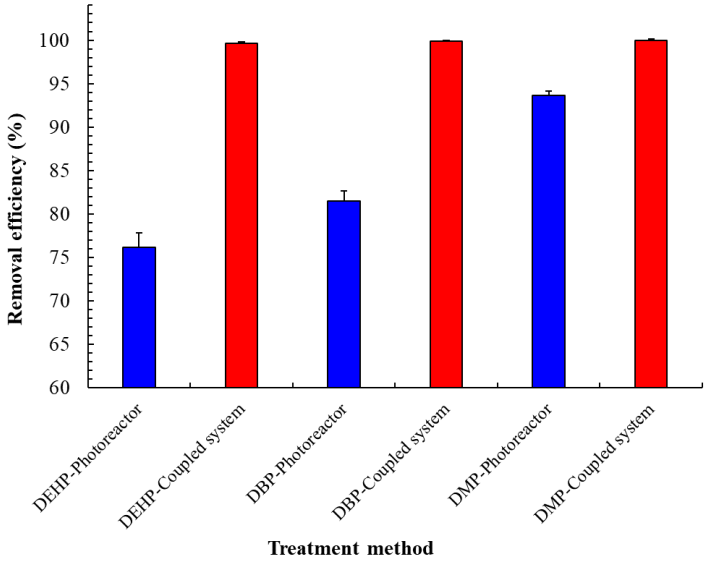

Figure 6. PAE removal efficiency of the visible-light photoreactor and developed coupled photobiological system from synthetic wastewater containing a PAE mixture (50 mg/L of DEHP, DBP, and DMP). Light intensity: 300 W; temperature: 30 °C; pH: 5.0; and RT: 5.5 min. The pH of the photoreactor effluent was automatically adjusted to 7.0 in the storage tank, and the effluent was then continuously piped into the PBR under an RT of 4 h.

4. Conclusions

The present study is the first to evaluate PAE mixtures by using a coupled visible-light photobiological system. The photocatalysis in the visible-light photoreactor follows first-order kinetics. Furthermore, the DEHP removal efficiency is affected considerably when another PAE mixture (DEHP, DBP, or DMP) simultaneously exists in the wastewater. When conducting photocatalytic pretreatment over a short period, an increase in the biodegradability of the effluent considerably improves the performance of the PBR. The developed coupled visible-light photobiological system considerably outperforms the UV photoreactor system alone in terms of the removal efficiency, energy consumption, and cost. The developed coupled photobiological system is feasible and promising for

continuously degrading PAEs in wastewater. The optimal parameters of the coupled visible-light photobiological system when incorporating direct sunlight in the photocatalysis of PAEs should be examined in a future study.

Author Contributions: Conceptualization, C.-Y.C. (Chih-Yu Chen), G.-H.W., and Y.-C.C.; methodology, Y.-J.C.; software, Y.-H.C.; validation, G.-H.W.; formal analysis, Y.-J.C.; investigation, Y.-H.C. and C.-Y.C. (Chiu-Yu Cheng); data curation, Y.-J.C., Y.-H.C., and C.-Y.C. (Chiu-Yu Cheng); writing—original draft preparation, C.-Y.C. (Chih-Yu Chen), G.-H.W., and Y.-C.C.; writing—review and editing, C.-Y.C. (Chih-Yu Chen) and Y.-C.C.; supervision, Y.-C.C.; project administration, Y.-C.C.; funding acquisition, C.-Y.C. (Chih-Yu Chen). All authors have read and agreed to the published version of the manuscript.

Funding: This research was funded by the Ministry of Science and Technology (Taiwan), grant number MOST 108-2637-B-266-001- and MOST 110-2637-B-266-001-.

Institutional Review Board Statement: Not applicable.

Informed Consent Statement: Not applicable.

Data Availability Statement: Not applicable.

Acknowledgments: The authors thank Chia-Chi Liang for help with the partially analytical measurements.

Conflicts of Interest: The authors declare no conflict of interest.

References

1. Das, M.T.; Kumar, S.S.; Ghosh, P.; Shah, G.; Malyan, S.K.; Bajar, S.; Thakur, I.S.; Singh, L. Remediation strategies for mitigation of phthalate pollution: Challenges and future perspectives. *J. Hazard. Mater.* **2021**, *409*, 124496. [CrossRef] [PubMed]
2. Xu, L.; Yang, X.; Guo, Y.; Ma, F.; Guo, Y.; Yuan, X.; Huo, M. Simulated sunlight photodegradation of aqueous phthalate esters catalyzed by the polyoxotungstate/titania nanocomposite. *J. Hazard. Mater.* **2010**, *178*, 1070–1077. [CrossRef] [PubMed]
3. Chang, B.V.; Wang, T.H.; Yuan, S.Y. Biodegradation of four phthalate esters in sludge. *Chemosphere* **2007**, *69*, 1116–1123. [CrossRef] [PubMed]
4. Chang, G.R.; Chen, H.S.; Chuang, W.C. Preliminary determination of phthalates in field vegetables and fruits in Taiwan. *Taiwan. J. Agric. Chem. Food. Sci.* **2016**, *54*, 212–217.
5. Lin, Z.; Zhang, W.; Zhu, X.; Wu, W.; Chen, Y.; Li, G.; Ren, L.; Luo, S.; Xie, Y.; Huang, Y.; et al. Effects of biochar pyrolysis temperature on di-2-ethylhexyl phthalate (DEHP) removal performance and microbial community structure in coastal sediments. *Environ. Technol. Inno.* **2021**, *24*, 102004. [CrossRef]
6. Huang, R.; Yan, H.; Li, L.; Deng, D.; Shu, Y.; Zhang, Q. Catalytic activity of Fe/SBA-15 for ozonation of dimethyl phthalate in aqueous solution. *Appl. Catal. B* **2011**, *106*, 264–271. [CrossRef]
7. Radke, E.G.; Glenn, B.S.; Braun, J.M.; Cooper, G.S. Phthalate exposure and female reproductive and developmental outcomes: A systematic review of the human epidemiological evidence. *Environ. Int.* **2019**, *130*, 104580. [CrossRef]
8. Wang, J.; Chen, L.; Shi, H.; Qian, Y. Microbial degradation of phthalic acid esters under anaerobic digestion of sludge. *Chemosphere* **2000**, *41*, 1245–1248.
9. Chen, C.Y.; Chen, C.C.; Chung, Y.C. Removal of phthalate esters by α-cyclodextrin-linked chitosan bead. *Bioresour. Technol.* **2007**, *98*, 2578–2583. [CrossRef]
10. Hung, C.H.; Yuan, C.; Li, H.W. Photodegradation of diethyl phthalate with PANi/CNT/TiO_2 immobilized on glass plate irradiated with visible light and simulated sunlight—effect of synthesized method and pH. *J. Hazard. Mater.* **2017**, *322*, 243–253. [CrossRef]
11. Wang, X.K.; Wang, C.; Jiang, W.Q.; Guo, W.L.; Wang, J.G. Sonochemical synthesis and characterization of Cl-doped TiO_2 and its application in the photodegradation of phthalate ester under visible light irradiation. *Chem. Eng. J.* **2012**, *189*, 288–294. [CrossRef]
12. Zolfaghari, M.; Drogui, P.; Seyhi, B.; Brar, S.K.; Buelna, G.; Dubé, R. Occurrence, fate and effects of di-(2-ethylhexyl) phthalate in wastewater treatment plants: A review. *Environ. Pollut.* **2014**, *194*, 281–293. [CrossRef] [PubMed]
13. Anandan, S.; Pugazhenthiran, N.; Lana-Villarreal, T.; Lee, G.J.; Wu, J.J. Catalytic degradation of a plasticizer, di-ethylhexyl phthalate, using N_x–TiO_{2-x} nanoparticles synthesized via co-precipitation. *Chem. Eng. J.* **2013**, *231*, 182–189. [CrossRef]
14. Chen, C.Y.; Wu, P.S.; Chung, Y.C. Coupled biological and photo-Fenton pretreatment system for the removal of di-(2-ethylhexyl) phthalate (DEHP) from water. *Bioresour. Technol.* **2009**, *100*, 4531–4534. [CrossRef] [PubMed]
15. Zhu, S.; Xia, M.; Chu, Y.; Khan, M.A.; Lei, W.; Wang, F.; Muhmood, T.; Wang, A. Adsorption and desorption of Pb (II) on l-lysine modified montmorillonite and the simulation of interlayer structure. *Appl. Clay Sci.* **2019**, *169*, 40–47. [CrossRef]
16. Štengl, V.; Grygar, T.M. The simplest way to iodine-doped anatase for photocatalysts activated by visible light. *Int. J. Photoenergy* **2011**, *2011*, 685935. [CrossRef]

17. Hong, X.; Wang, Z.; Cai, W.; Lu, F.; Zhang, J.; Yang, Y.; Ma, N.; Liu, Y. Visible-light-activated nanoparticle photocatalyst of iodine-doped titanium dioxide. *Chem. Mater.* **2005**, *17*, 1548–1552. [CrossRef]
18. Chen, C.Y.; Wang, G.H.; Tseng, I.H.; Chung, Y.C. Analysis of bacterial diversity and efficiency of continuous removal of Victoria Blue R from wastewater by using packed-bed bioreactor. *Chemosphere* **2016**, *145*, 17–24. [CrossRef]
19. Chung, Y.C.; Chen, C.Y. Degradation of di-(2-ethylhexyl) phthalate (DEHP) by TiO_2 photocatalysis. *Water Air Soil Pollut.* **2009**, *200*, 191–198. [CrossRef]
20. Zhang, X.; Feng, M.; Qu, R.; Liu, H.; Wang, L.; Wang, Z. Catalytic degradation of diethyl phthalate in aqueous solution by persulfate activated with nano-scaled magnetic $CuFe_2O_4$/MWCNTs. *Chem. Eng. J.* **2016**, *301*, 1–11. [CrossRef]
21. Zhang, Y.; Yu, H.; Li, S.; Wang, L.; Huang, F.; Guan, R.; Li, J.; Jiao, Y.; Sun, J. Rapidly degradation of di-(2-ethylhexyl) phthalate by Z-scheme Bi_2O_3/TiO_2 reduced graphene oxide driven by simulated solar radiation. *Chemosphere* **2021**, *272*, 129631. [CrossRef] [PubMed]
22. Kanaujiya, D.K.; Sivashanmugam, S.; Pakshirajan, K. Biodegradation and toxicity removal of phthalate mixture by *Gordonia* sp. in a continuous stirred tank bioreactor system. *Environ. Technol. Innov.* **2022**, *26*, 102324. [CrossRef]
23. Kaneco, S.; Katsumata, H.; Suzuki, T.; Ohta, K. Titanium Dioxide mediated photocatalytic degradation of dibutyl phthalate in aqueous solution—kinetics, mineralization and reaction mechanism. *Chem. Eng.* **2006**, *125*, 59–66. [CrossRef]
24. Zhang, H.; Lin, Z.; Liu, B.; Wang, G.; Weng, L.; Zhou, J.; Hu, H.; He, H.; Huang, Y.; Chen, J.; et al. Bioremediation of di-(2-ethylhexyl) phthalate contaminated red soil by *Gordonia terrae* RL-JC02: Characterization, metabolic pathway and kinetics. *Sci. Total Environ.* **2020**, *733*, 139138. [CrossRef] [PubMed]
25. Zhao, H.; Du, H.; Feng, N.; Xiang, L.; Li, Y.; Li, H.; Cai, Q.; Mo, C. Biodegradation of di-*n*-butylphthalate and phthalic acid by a novel *Providencia* sp. 2D and its stimulation in a compost-amended soil. *Biol. Fertil. Soils* **2016**, *52*, 65–76. [CrossRef]
26. Feng, N.; Yu, J.; Mo, C.; Zhao, H.; Li, Y.; Wu, B. Biodegradation of di-*n*-butyl phthalate (DBP) by a novel endophytic *Bacillus megaterium* strain YJB3. *Sci. Total Environ.* **2018**, *616–617*, 117–127. [CrossRef]
27. Singh, T.; Suman, S.; Rashmi, M.; Singh, A. Biodegradation of di-(2-Ethylhexyl Phalate) by *Bacillus antracis* (Accession no. KJ085972.1). *J. Ecophysiol. Occup. Health* **2020**, *20*, 140–144. [CrossRef]
28. Hashizume, K.; Nanya, J.; Toda, C.; Yasui, T.; Nagano, H.; Kojima, N. Phthalate esters detected in various water samples and biodegradation of the phthalates by microbes isolated from river water. *Biol. Pharm. Bull.* **2002**, *25*, 209–214. [CrossRef]
29. Abioye, P.O.; Iroegu, V.T.; Abiodun, A.S. Biodegradation of methyl red by *Staphylococcus aureus* isolated from waste dump site. *J. Environ. Sci. Technol.* **2015**, *8*, 131–138. [CrossRef]
30. Sahasrabudhe, M.M.; Saratale, R.G.; Saratale, G.D.; Pathade, G.R. Decolorization and detoxification of sulfonated toxic diazo dye C.I. Direct Red 81 by *Enterococcus faecalis* YZ 66. *J. Environ. Health Sci. Eng.* **2014**, *12*, 151. [CrossRef]
31. Bai, N.; Li, S.; Zhang, J.; Zhang, H.; Zhang, H.; Zheng, X.; Lv, W. Efficient biodegradation of DEHP by CM9 consortium and shifts in the bacterial community structure during bioremediation of contaminated soil. *Environ. Pollut.* **2020**, *266 Pt 2*, 115112. [CrossRef]
32. Nshimiyimana, J.B.; Khadka, S.; Zou, P.; Adhikari, S.; Proshad, R.; Thapa, A.; Xiong, L. Study on biodegradation kinetics of di-2-ethylhexyl phthalate by newly isolated halotolerant *Ochrobactrum anthropi* strain L1-W. *BMC Res. Notes* **2020**, *13*, 252. [CrossRef] [PubMed]
33. Zeng, F.; Cui, K.; Li, X.; Fu, J.; Sheng, G. Biodegradation kinetics of phthalate esters by *Pseudomonas fluoresences* FS1. *Process. Biochem.* **2004**, *39*, 1125–1129. [CrossRef]
34. Heydarnezhad, F.; Hoodaji, M.; Shahriarinour, M.; Tahmourespour, A. Toluene degradation by free *Staphylococcus gallinarum* and immobilized on multi-walled carbon nanotubes. *Front. J. Soc. Technol. Environ. Sci.* **2021**, *10*, 61–73. [CrossRef]
35. Peng, X.; Qu, X.; Luo, W.; Jia, X. Bioresource technology co-metabolic degradation of tetrabromobisphenol a by novel strains of *Pseudomonas* sp. and *Streptococcus* sp. *Bioresour. Technol.* **2014**, *169*, 271–276. [CrossRef] [PubMed]
36. Hassan, M.M.; Alam, M.Z.; Anwar, M.N. Biodegradation of textile azo dyes by bacteria isolated from dyeing industry effluent. *Int. Res. J. Biological Sci.* **2013**, *2*, 27–31.
37. Yang, T.; Ren, L.; Jia, Y.; Fan, S.; Wang, J.; Wang, J.; Nahurira, R.; Wang, H.; Yan, Y. Biodegradation of di-(2-ethylhexyl) phthalate by *Rhodococcus ruber* YC-YT1 in contaminated water and soil. *Int. J. Environ. Res. Public Health* **2018**, *15*, 964. [CrossRef]
38. Wright, R.J.; Bosch, R.; Gibson, M.I.; Christie-Oleza, J.A. Plasticizer degradation by marine bacterial isolates: A proteogenomic and metabolomic characterization. *Environ. Sci. Technol.* **2020**, *54*, 2244–2256. [CrossRef]
39. Pradeep, S.; Sarath Josh, M.K.; Binod, P.; Sudha Devi, R.; Balachandran, S.; Anderson, R.C.; Benjamin, S. *Achromobacter denitrificans* strain SP1 efficiently remediates di(2-ethylhexyl)phthalate. *Ecotoxicol. Environ. Saf.* **2015**, *112*, 114–121. [CrossRef]
40. Hu, R.; Zhao, H.; Xu, X.; Wang, Z.; Yu, K.; Shu, L.; Yan, Q.; Wu, B.; Mo, C.; He, Z.; et al. Bacteria-driven phthalic acid ester biodegradation: Current status and emerging opportunities. *Environ. Int.* **2021**, *154*, 106560. [CrossRef]
41. Chao, W.L.; Cheng, C.Y. Effect of introduced phthalate-degrading bacteria on the diversity of indigenous bacterial communities during di-(2-ethylhexyl) phthalate (DEHP) degradation in a soil microcosm. *Chemosphere* **2007**, *67*, 482–488. [CrossRef] [PubMed]
42. Li, J.; Zhang, J.; Yadav, M.P.; Li, X. Biodegradability and biodegradation pathway of di-(2-ethylhexyl) phthalate by *Burkholderia pyrrocinia* B1213. *Chemosphere* **2019**, *225*, 443–450. [CrossRef] [PubMed]
43. Gao, D.W.; Wen, Z.D. Phthalate esters in the environment: A critical review of their occurrence, biodegradation, and removal during wastewater treatment processes. *Sci. Total Environ.* **2016**, *541*, 986–1001. [CrossRef] [PubMed]